Detecting Low-Power RF Signals Using a Multimode Optoelectronic Oscillator and Integrated Optical Filter

Preetpaul S. Devgan, *Member, IEEE*, Marcel W. Pruessner, *Member, IEEE*, Vincent J. Urick, *Member, IEEE*, and Keith J. Williams, *Member, IEEE*

***Abstract*—We have assembled and characterized a multimode optoelectronic oscillator with integrated optical filter for detecting low-power radio-frequency (RF) signals. The system can selectively amplify RF signals from 1 to 6 GHz. The input signals can be as low as −83 dBm with a compression dynamic range of 72 dB. Using an integrated silicon optical filter facilitates channelization of the amplified RF signal from 1 to 3 GHz by reducing the gain for signals above 3 GHz. Future system improvements are discussed.**

***Index Terms*—Channelization, optoelectronic oscillator (OEO), silicon integrated optical filters.**

I. Introduction

THE ability to detect very low-power radio-frequency (RF) signals in a cluttered environment is important in applications such as radio astronomy [1] and channelization [2]. For these applications, it is important to not only determine the frequency of the signal but also to amplify the signal. Photonic techniques are preferred for performing these applications as they have broad instantaneous bandwidths. While demonstrations have been proposed to detect RF frequencies in a noisy environment using dispersion [3] or narrowband optical filters [4], these methods have not focused on selectively amplifying very low-power RF signals. A new method that can be used to detect and amplify low RF power signals uses a multimode optoelectronic oscillator (OEO). While single-mode OEOs have been well-studied for RF signal recovery through the injection-locking process [5], [6], the use of a multimode OEO has not been fully explored. A multimode OEO differs from a typical OEO in that there is no electrical bandpass filter inside the OEO cavity. Typically, the recovered RF signal is limited to a narrow frequency range set by the filter. On the other hand, the multimode OEO can be injection-locked to any incoming frequency that matches the free-running modes of the cavity. By keeping the gain in the OEO just below threshold, a cavity mode can only oscillate if an appropriate external signal is introduced. This condition allows the OEO to selectively amplify very low-power signals while providing loss to signals outside the cavity modes. We recently demonstrated a multimode OEO using an intracavity RF amplifier that gives 10-dB gain at 1 GHz to signals that meet the mode condition of the cavity while providing 10 dB of loss when the injected signal is outside the cavity mode [7]. However, the noise from the RF amplifier reduces the sensitivity of the system. Using an all-optical gain multimode OEO can address this issue. In addition, using narrowband integrated optical filters [8] at the output of the multimode OEO allows for narrow frequency bands to be separately monitored.

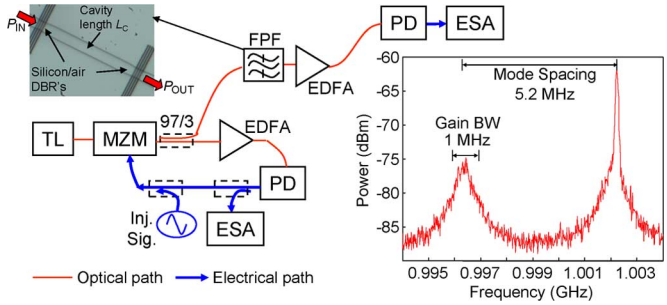

Fig. 1. OEO setup for selective amplification and detection along with measured output of OEO for a −70-dBm injected signal at 1.0022 GHz. The gain bandwidth at a single mode is 1 MHz. PD: photodiode; TL: tunable laser.

We have built a multimode OEO in order to detect and amplify very low-power RF signals over a frequency range from 1 to 6 GHz. The system selectively provides gain to RF frequencies that match the cavity modes of the OEO. We have characterized the system's sensitivity, dynamic range, and resistance to large signals. In addition, we have added an integrated Fabry–Pérot optical filter to allow us to operate over a 3-GHz RF span without interference from out-of-band signals. The filters can be scaled up to many devices on a chip, thereby facilitating future systems for RF channelization.

II. Multimode Optoelectronic Oscillator

The multimode OEO in Fig. 1 consists of a tunable laser that is followed by a Mach–Zehnder modulator (MZM). A 97%/3% coupler is used after the MZM to send some of the signal through the Fabry–Pérot filter (FPF). The 97% output is connected to an erbium-doped fiber amplifier (EDFA) and the amplified signal is sent to a photodetector. Part of the detected electrical signal is measured with an electrical spectrum analyzer (ESA). The rest of the signal is fed via a coupler into the RF port of the MZM. The other coupler port is used to inject an

Manuscript received August 10, 2009; accepted November 07, 2009. First published December 01, 2009; current version published January 13, 2010.

The authors are with the U.S. Naval Research Laboratory, Washington, DC 20375 USA (e-mail: pdevgan@ccs.nrl.navy.mil; marcel.pruessner@nrl.navy.mil; vurick@ccs.nrl.navy.mil; keith.williams@nrl.navy.mil).

Color versions of one or more of the figures in this letter are available online at http://ieeexplore.ieee.org.

Digital Object Identifier 10.1109/LPT.2009.2037154

Report Documentation Page

Form Approved
OMB No. 0704-0188

1. REPORT DATE	2. REPORT TYPE	3. DATES COVERED
01 FEB 2010		**00-00-2010 to 00-00-2010**

4. TITLE AND SUBTITLE	5a. CONTRACT NUMBER
Detecting Low-Power RF Signals Using a Multimode Optoelectronic Oscillator and Integrated Optical Filter	5b. GRANT NUMBER
	5c. PROGRAM ELEMENT NUMBER
6. AUTHOR(S)	5d. PROJECT NUMBER
	5e. TASK NUMBER
	5f. WORK UNIT NUMBER
7. PERFORMING ORGANIZATION NAME(S) AND ADDRESS(ES) **U.S. Naval Research Laboratory,Washington,DC**	8. PERFORMING ORGANIZATION REPORT NUMBER
9. SPONSORING/MONITORING AGENCY NAME(S) AND ADDRESS(ES)	10. SPONSOR/MONITOR'S ACRONYM(S)
	11. SPONSOR/MONITOR'S REPORT NUMBER(S)

12. DISTRIBUTION/AVAILABILITY STATEMENT
Approved for public release; distribution unlimited

13. SUPPLEMENTARY NOTES

14. ABSTRACT

15. SUBJECT TERMS

16. SECURITY CLASSIFICATION OF:			17. LIMITATION OF ABSTRACT	18. NUMBER OF PAGES	19a. NAME OF RESPONSIBLE PERSON
a. REPORT	b. ABSTRACT	c. THIS PAGE			
unclassified	**unclassified**	**unclassified**	**Same as Report (SAR)**	**3**	

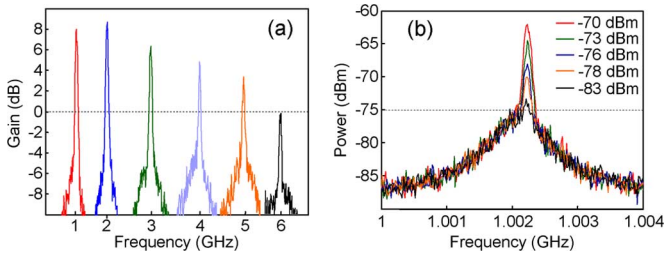

Fig. 2. (a) RF gain for signals from 1 to 6 GHz. (b) OEO sensitivity to low power input RF signals before reaching noise floor at −75 dBm.

external signal into the OEO cavity. Our system differs from a traditional OEO in two ways: first, the electrical bandpass filter is removed, allowing the OEO to run multimode and second, the length of fiber in the OEO is minimized, separating the cavity modes as far apart as possible. With the intracavity gain kept just below threshold, no single mode can oscillate over the other modes, allowing the OEO to remain sensitive to an external injected signal. Here, the OEO operates 1 dB below threshold at 1 GHz with a photocurrent of 20.2 mA. The mode spacing is 5.2 MHz, limited by the long length of fiber in the EDFA.

We inject a 1.0022-GHz signal into the cavity. The frequency is chosen to match one of the cavity modes of the OEO (Fig. 1). The floor due to the nonoscillating mode is around −75 dBm, while the amplified signal is measured at −62 dBm. The RF power of the input signal is −70 dBm, yielding a gain of 8 dB. To measure the bandwidth of the gain at a single mode, the power of the injected signal is set to −70 dBm and the frequency is tuned from the peak of the gain until the signal sees zero gain. The tuning range is measured to be +/−500 kHz. Outside of this bandwidth, the signal power remained below the cavity mode power until the signal frequency was swept to the next cavity mode 5.2 MHz away. The selective amplification allows the OEO to discern between signals of interest within a 1-MHz band around a given frequency; the peak of individual gain channels are spaced 5.2 MHz away. We repeat the measurement for input frequencies from 2 to 6 GHz and the same 1-MHz bandwidth is observed. To measure the overall bandwidth of the system, the input RF signal is tuned to the nearest cavity mode in 1-GHz steps until the gain was less than unity [Fig. 2(a)]. The gain of the system increases around 2 GHz and then slowly rolls down to 0 dB at 6 GHz. The gain increase from 1 to 2 GHz is consistent with the frequency dependence of the coupler, whose operating bandwidth is 2–18 GHz. The roll-off is consistent with the loss of the OEO cavity due mostly to the frequency-dependent V_π of the MZM.

The input signal is decreased until the resulting signal cannot be distinguished from the cavity mode, in order to determine how low the input signal can still be observed above the cavity mode noise floor [Fig. 2(b)]. The input signal is above the cavity mode floor until an input power of −83 dBm. This same measurement was made for frequencies ranging from 2 to 6 GHz. The lowest detectable input power changes from −83 dBm (at 2 GHz) up to −75 dBm (at 6 GHz). Again the change is consistent with the measured frequency loss of the cavity.

Next, we studied how the system operates when there is a very large signal at the next cavity mode to the small signal of interest. When a large signal is injected into the cavity, it may dominate the gain of the cavity and the smaller signal of interest will not be amplified. In order to determine the negative effect of a large signal in the next frequency mode, a large power second signal is injected at the frequency mode adjacent to the small signal frequency. The results for the 1-GHz signal are shown in Fig. 3. As the power of the second signal is increased, the low power signal stays the same, until the power of the second signal reaches −11 dBm. At this point, the small signal output power begins to drop. We verify that this is due to the MZM by performing a measurement of the MZM compression inside the OEO loop. The measurement appears as an inset in Fig. 3. The input power where the MZM gain is no longer linear is the same at the point that the injected signal causes the smaller signal to attenuate. Again these measurements were made in the 2- to 6-GHz range and the results are consistent with the 1-GHz case. Since there is no RF amplifier in our cavity, the MZM is the first component to compress and allows us to operate at an input power range from −83 to −11 dBm, which yields a compression dynamic range of 72 dB.

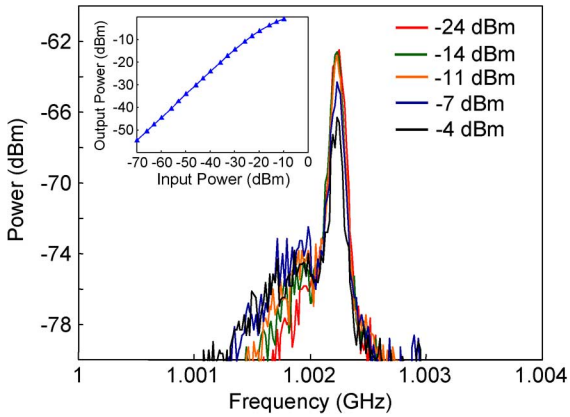

Fig. 3. OEO gain degradation due to large signals at the next mode of the signal of interest. Inset: RF power compression for MZM at 1 GHz.

The system described above has enabled us to detect small RF signals covering a large RF band. In order to measure a single (or multiple) frequency band(s) for channelization of an RF spectrum, we make use of the FPF in Fig. 1. The purpose of the integrated optical bandpass filter is to narrow the RF bandwidth in order to reject out-of-band OEO cavity modes by suppressing their gain below 0 dB.

III. Integrated FPF

The integrated microcavity filters consist of silicon-on-insulator rib waveguides with distributed Bragg reflector (DBR) gratings that form a Fabry–Pérot resonator. The DBR's consist of $\lambda/4$ wide air trenches etched into the silicon. The large silicon/air refractive index contrast $(\Delta n = 3.48)$ enables mirrors with high reflectance using only a few air gaps. We designed DBR mirrors with reflectance $R = 0.9074, 0.9892, 0.9974$ for two, three, and four air gaps, respectively. While previous filters had short cavities (cavity length $L_C = 12$ μm [8]), the current filters have a $L_C = 500$ μm and high Q.

The measured transmission spectrum for a three air gap filter is shown in Fig. 4(a) for $\lambda = 1540 - 1560$ nm. The large

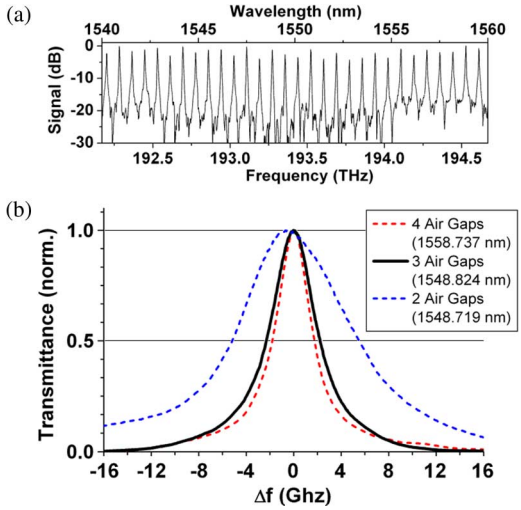

Fig. 4. Measured silicon FPF response for $L_C = 500\ \mu$m long cavity: (a) response for three-air gap DBR filter over wavelength $\lambda = 1540 - 1560$ nm, (b) resonance bandwidth for two, three, and four air-gap DBR filters near $\lambda = 1550$ nm ($\mathrm{BW}_{3\ \mathrm{dB}} = 10.5,\ 4.5,$ and 3.5 GHz, respectively).

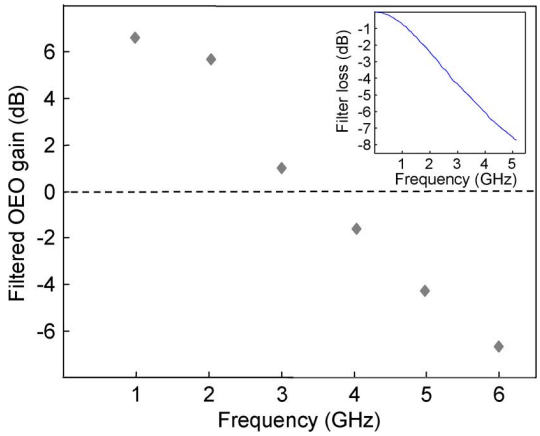

Fig. 5. OEO gain after passing through FPF over 1- to 6-GHz range. Inset: frequency response of the FPF.

free-spectral range FSR ≈ 0.664 nm (83 GHz) at $\lambda \approx 1550$ nm is possible due to the relatively short cavity length compared to all-fiber cavities. The filter rejection is -25 dB. For the two air gap filter, the insertion loss is 2.0 dB compared to a test waveguide on-chip; devices with three and four air gaps exhibit higher insertion loss due to the increased DBR reflectance and scattering loss in the air gaps. Fig. 4(b) compares several filter bandwidths measured near $\lambda \approx 1550$ nm. Consistent with finite-difference time-domain (FDTD) simulations, DBRs with larger number of air gaps result in higher mirror reflectance and hence sharper filter resonances: we measure a 3-dB bandwidth $\mathrm{BW}_{3\ \mathrm{dB}} = 10.5$ GHz ($Q = 18\,500$), 4.5 GHz (43 000), and 3.5 GHz (55 000) for two, three, and four air gaps, respectively. The BW narrows only slightly by going from three to four air gaps, which indicates that scattering and diffraction losses dominate over the increased DBR reflectance.

We inserted a filter with BW $= 4.5$ GHz at the 3% output of the OEO cavity, as shown in Fig. 1. We chose this device in favor of the narrower BW $= 3.5$ GHz device since it exhibited lower insertion loss. The optical signal after the filter is then amplified by an EDFA and measured at an ESA. The RF gain of the different RF tones was measured as a function of frequency. These results appear in Fig. 5. The filter loss, along with the gain roll-off of the OEO [see Fig. 2(a)], reduces the RF gain from the OEO to less than 1 dB at 3 GHz. Thus the filter can be used to remove the gain of the OEO for signals above 3 GHz, allowing us to narrow the gain bandwidth. By extending these results to single-chip integrated filter arrays, we can cover multiple bands in a large RF spectrum towards narrowband frequency channelization.

IV. Conclusion

Our multimode OEO exhibits gains up to 8 dB for signals at -70 dBm and has gain for signals up to 6 GHz. The system's sensitivity is -83 dBm and the compression dynamic range 72 dB. Combining the OEO with an integrated optical filter allows us to narrow the RF gain bandwidth. The filter removes the gain of the OEO for signals at 3 GHz and above. Future work aims to improve the system by replacing the EDFA with a semiconductor optical amplifier (SOA), which significantly reduces the length of the OEO cavity and increases the mode spacing to >5.2 MHz. New filters are also being developed with expected BW ≤ 1 GHz to selectively pick out each mode of the OEO and allow for channelization of individual RF signals. The single OEO-filter system can be scaled up to incorporate multiple OEOs along with integrated silicon chips containing as many as 100 filters per chip to achieve true channelization of a large RF spectrum.

References

[1] J. Raza, A.-J. Boonstra, and A.-J. van der Veen, "Spatial filtering of RF interference in radio astronomy," *IEEE Sig. Process. Lett.*, vol. 9, no. 2, pp. 64–67, Feb. 2002.

[2] G. W. Anderson, D. C. Webb, A. E. Spezio, and J. N. Lee, "Advanced channelization for RF, microwave and millimeterwave applications," *Proc. IEEE*, vol. 79, pp. 355–388, 1991.

[3] L. V. T. Nguyen, "Microwave photonic technique for frequency measurement of simultaneous signals," *IEEE Photon. Technol. Lett.*, vol. 21, no. 10, pp. 642–644, May 15, 2009.

[4] M. S. Rasras, D. M. Gill, S. S. Patel, K.-Y. Tu, Y.-K. Chen, A. E. White, A. T. S. Pomerene, D. N. Carothers, M. J. Grove, D. K. Sparacin, J. Michel, M. A. Beals, and L. C. Kimerling, "Demonstration of a fourth-order pole-zero optical filter integrated using CMOS processes," *J. Lightw. Technol.*, vol. 25, no. 1, pp. 87–92, Jan. 2007.

[5] J. Lasri, P. Devgan, R. Tang, and P. Kumar, "Ultralow timing jitter 40-Gb/s clock recovery using a self-starting optoelectronic oscillator," *IEEE Photon. Technol. Lett.*, vol. 16, no. 1, pp. 263–265, Jan. 2004.

[6] M. Tsuchida and M. Suzuki, "40 Gb/s optical clock recovery using an injection-locked optoelectronic oscillator," *IEEE Photon. Technol. Lett.*, vol. 17, no. 1, pp. 211–213, Jan. 2005.

[7] V. J. Urick, P. S. Devgan, J. D. McKinney, F. Bucholtz, and K. J. Williams, "Channelisation of radio-frequency signals using an optoelectronic oscillator," *Electron. Lett.*, vol. 45, no. 24, pp. 1242–1244, Nov. 2009.

[8] M. W. Pruessner, T. H. Stievater, and W. S. Rabinovich, "Integrated waveguide Fabry-Perot microcavities with silicon/air Bragg mirrors," *Opt. Lett.*, vol. 32, no. 5, pp. 533–535, 2007.